Accepted Manuscript

A $NaAlH_4$-$Ca(BH_4)_2$ composite system for hydrogen storage

Kasper T. Møller, Jakob B. Grinderslev, Torben R. Jensen

PII: S0925-8388(17)31881-9

DOI: 10.1016/j.jallcom.2017.05.264

Reference: JALCOM 41995

To appear in: *Journal of Alloys and Compounds*

Received Date: 26 April 2017

Revised Date: 19 May 2017

Accepted Date: 25 May 2017

Please cite this article as: K.T. Møller, J.B. Grinderslev, T.R. Jensen, A $NaAlH_4$-$Ca(BH_4)_2$ composite system for hydrogen storage, *Journal of Alloys and Compounds* (2017), doi: 10.1016/j.jallcom.2017.05.264.

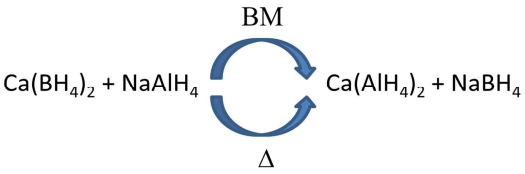

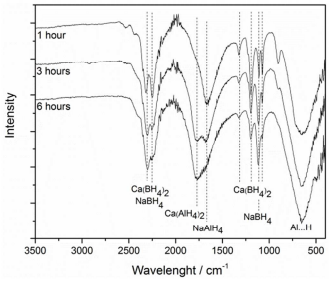

A $NaAlH_4$-$Ca(BH_4)_2$ Composite System for Hydrogen Storage

Kasper T. Møller,[1] Jakob B. Grinderslev,[1] Torben R. Jensen. [1*]

[1]*Interdisciplinary Nanoscience Center (iNANO) and Department of Chemistry, University of Aarhus, DK-8000 Aarhus, Denmark*

This paper has been presented in Symposium O: Functional metal hydrides, at the E-MRS Fall Meeting and Exhibit, Warsaw, September, 2016.

*Corresponding Author

Torben R. Jensen

trj@chem.au.dk

Center for Materials Crystallography

iNANO and Department of Chemistry

Langelandsgade 140

D-8000 Aarhus C

Aarhus University

Denmark

Keywords: hydrogen storage, reactive hydride composites, sodium alanate, calcium alanate.

Abstract

Mechanochemical treatment (ball-milling) of $NaAlH_4$-$Ca(BH_4)_2$ mixtures leads to partial formation of $NaBH_4$ and $Ca(AlH_4)_2$ by a metathesis reaction. The reaction proceeds to different extents depending on the applied ball-milling times, which is confirmed by powder X-ray diffraction and infrared spectroscopy. Additionally, an *in-situ* synchrotron radiation powder X-ray diffraction study reveals that the metathesis reaction continues due to thermal treatment while the data also supports a two-step decomposition of the formed $Ca(AlH_4)_2$. Finally, the reactive hydride composite system was investigated by mass spectrometry and Sieverts' measurement, which reveal release of ~6 wt% H_2 at T < 375 °C.

1. Introduction

An efficient energy storage system where large amounts of renewable energy can be stored is generally pursued *e.g.* concentrating solar thermal power plants or as hydrogen [1,2]. An energy storage system can level out the intermittent supply of renewable energy to match our oscillating energy demand and also be used for mobile applications [3–5]. Thus, hydrogen as an energy carrier has been considered for decades now owing to its unique properties *e.g.* the high gravimetric energy density of ~120 kJ/g (lower heating value) [1,3]. The discovery of the reversible $NaAlH_4$-$TiCl_3$ hydrogen storage system led to significantly increased interest in complex metal hydrides [6]. Among them, $Ca(BH_4)_2$, with a gravimetric hydrogen density of ρ_m = 11.6 wt%, has been thoroughly studied [7–10]. On the other hand, calcium alanate, $Ca(AlH_4)_2$, ρ_m = 7.9 wt%, is a less studied metal alanate [11,12].

A combination of the two well studied compounds, $NaAlH_4$ and $Ca(BH_4)_2$, is the focus of the present investigation. The reactive hydride composite, $NaAlH_4$-$Ca(BH_4)_2$, contains 9.77 wt% of

hydrogen and is thus worth attention. Previously, similar composite systems of $NaAlH_4$-$LiBH_4$ and $NaAlH_4$-$Mg(BH_4)_2$ have been investigated with the formation of $NaBH_4$ and $LiAlH_4$ or $Mg(AlH_4)_2$, respectively, as a result [13–15]. Additionally, mechanochemical and solvent mediated synthesis of $Ca(AlH_4)_2$ has been performed from CaH_2 and AlH_3 or $NaAlH_4$ and $CaCl_2$ [11,12,16,17]. However, the formation of salts *e.g.* NaCl decreases the hydrogen capacity of the reactive hydride composite.

In this work, the reactive hydride composite $NaAlH_4$-$Ca(BH_4)_2$ has been studied with the outcome of formation of $Ca(AlH_4)_2$ and $NaBH_4$. The composite has been studied in detail by *in-situ* synchrotron radiation powder X-ray diffraction, Fourier transformed infrared spectroscopy and mass spectrometry. The reaction between $NaAlH_4$ and $Ca(BH_4)_2$ is not only mechanically induced but continues during thermal treatment.

2. Experimental

2.1 Sample preparation. $Ca(BH_4)_2$ was synthesized from commercially available CaH_2 (Sigma Aldrich, reagent grade, 95%) and a borane dimethyl sulphide complex (DMS-BH_3, Sigma-Aldrich) which was stirred together for ~2 days at T = 40 °C using a similar approach as to synthesize $Sr(BH_4)_2$ [18]. Finally, the solution was dried under vacuum at room temperature (*RT*) on a Schlenk line. The final product was confirmed by powder X-ray diffraction to be α-$Ca(BH_4)_2$.

$NaAlH_4$ (Sigma-Aldrich, Tech. grade) and the as-synthesized $Ca(BH_4)_2$ in a 1:1 ratio were treated mechanochemically in the Fritsch Pulverisette 6 in WC vials (80 mL) with WC balls (d = 8 mm) under an argon atmosphere with a ball-to-powder mass ratio of 40. The powder was ball-milled for 5 minutes at 350 rpm followed by a break of 3 minutes, to prevent sample overheating and possible decomposition of products. The milling program was repeated 12, 36 or 72 times to establish an effective ball-milling time of 1, 3 or 6 hours, respectively.

2.2 Powder X-ray Diffraction (PXD). PXD data of as-prepared samples were measured on a Rigaku Smart Lab diffractometer using a Cu source and a convergent beam mirror (Cu $K_{\alpha 1}$

radiation, λ = 1.540593 Å). Data were collected in the 2θ-range 10° to 80° at 2.5°/min using a Rigaku D/tex detector. All samples were mounted in an argon-filled glovebox in 0.5 mm glass capillaries sealed with glue.

2.3 Fourier-transform Infrared Spectroscopy (FT-IR). All as-milled samples were characterized by infrared absorption spectroscopy using a NICOLET 380 FT-IR spectrometer from Thermo Electron Corporation. Data were measured in the range 4000 – 400 cm^{-1} and 32 scans with a spectral resolution of 4 cm^{-1} were collected per sample and averaged. The samples were exposed to air for approximately 15 s when transferring the powder from the sample vial to the instrument.

2.4 *In-Situ* Synchrotron Radiation Powder X-ray Diffraction (SR-PXD). *In-situ* time-resolved SR-PXD data were collected at beamline I11 at Diamond Light Source, Oxford, UK, utilizing a wide-angle position sensitive detector (PSD) based on Mythen-2 Si strip modules, λ = 0.8258 Å. The powdered sample was packed in a 0.5 mm quartz capillary in an argon-filled glovebox (O_2, H_2O < 1 ppm) and rotated during measurement. Additionally, the sample was heated from *RT* to 400 °C ($\Delta T/\Delta t$ = 10 °C/min) using a heat blower available at I11 and the temperature of the sample was calibrated using NaCl as a standard [19,20].

2.5 Mass Spectrometry. Mass spectrometry (MS) analysis of the evolved gas was performed using a Hiden Analytical HPR-20 QMS sampling system. Approx. 8 mg of sample was loaded in an argon glovebox into a Al_2O_3 crucible and sealed with a Al_2O_3 lid. The samples were heated from 30 to 450 °C ($\Delta T/\Delta t$ = 5 °C/min) in an argon flow of 40 mL/min and the evolved gas was analyzed for hydrogen.

2.6 Sieverts' Measurement. The samples were desorbed in a stainless steel high-temperature autoclave attached to a custom made Sieverts apparatus [21]. The desorptions were carried out by heating the sample from *RT* to 450 °C ($\Delta T/\Delta t$ = 3 °C /min, $p(H_2)$ = 1 bar) and keeping it isothermal at 450 °C for 30 min. Subsequently, the sample was naturally cooled to *RT*.

3. Results and Discussion

3.1 Powder X-ray Diffraction

Figure 1 shows the PXD patterns of the as-milled $NaAlH_4$-$Ca(BH_4)_2$ samples. In the diffraction pattern of the 1 hour ball-milled sample, predominantly both starting reactants are present. However, as the ball-milling time is increased to 3 hours, Bragg reflections belonging to $NaBH_4$ appear and they become more significant after 6 hours of millinge. Meanwhile, the intensity of Bragg reflections from $NaAlH_4$ and, to some extent, $Ca(BH_4)_2$, decreases.

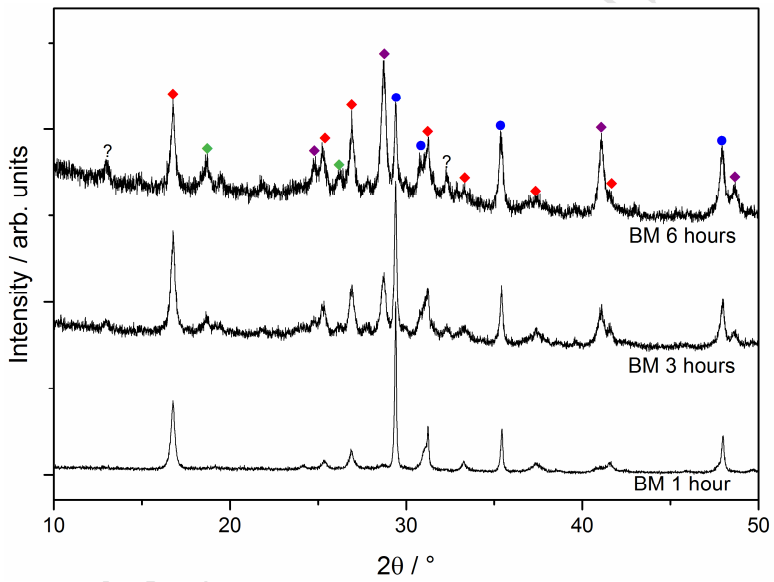

Figure 1. Powder X-ray diffraction data of the $NaAlH_4$–$Ca(BH_4)_2$ samples after different degrees of mechanochemical treatment (λ = 1.5406 Å). Markers: Red diamonds: α-$Ca(BH_4)_2$, green diamonds: β-$Ca(BH_4)_2$, purple diamonds: $NaBH_4$, blue spheres: $NaAlH_4$.

This tendency points towards the following metathesis reaction during mechanochemical treatment:

$$2NaAlH_4\ (s) + Ca(BH_4)_2\ (s) \rightarrow 2NaBH_4\ (s) + Ca(AlH_4)_2\ (s) \qquad \textbf{(1)}$$

which is further supported by the absence of Bragg reflections from NaH, CaH_2, CaB_6, and Al in the diffraction patterns. Thus, the complex hydrides, $NaAlH_4$, $NaBH_4$, $Ca(BH_4)_2$ and $Ca(AlH_4)_2$ appear not to decompose during mechanochemical treatment.

Finally, the $Ca(AlH_4)_2$ formed seems to be unstable over time as PXD after 10 months shows the presence of Al, as seen in Figure S1. Possibly, CaH_2 is present too, however, the most intense Bragg reflections from CaH_2 overlap with the Bragg reflections of $NaAlH_4$ and $NaBH_4$ and it is thus uncertain.

3.2 Infrared spectroscopy

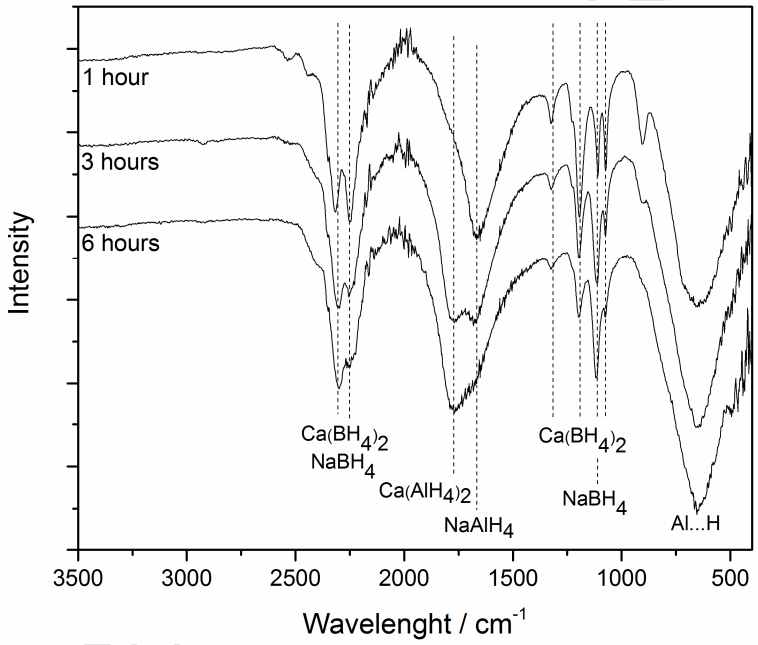

Figure 2. FT-IR spectra of $NaAlH_4$-$Ca(BH_4)_2$ ball-milled at different ball-milling times.

Infrared spectroscopy data is presented in Figure 2. The data reveals two B···H stretches at 2300 and 2255 cm^{-1} originating from both $Ca(BH_4)_2$ and $NaBH_4$, as the stretching modes overlap, and two Al···H stretches at 1783 and 1674 cm^{-1} assigned to $Ca(AlH_4)_2$ and $NaAlH_4$, respectively [11,22]. Furthermore, B···H bending modes are observed between 1195 and 1075 cm^{-1} while Al···H stretches are present at around 650 cm^{-1}. Interestingly, the ratio between the signal of $Ca(AlH_4)_2$ and $NaAlH_4$ changes in favour of $Ca(AlH_4)_2$ as the ball-milling time is increased. Meanwhile, the intensity of the

stretching mode at 2300 cm^{-1} and the bending mode at 1118 cm^{-1}, which are the most intense modes of $NaBH_4$ [22], increases. These observations are in agreement with the evolution of more $NaBH_4$ formed as milling-time is increased as observed in PXD. Hence, reaction **1** occurs to a larger extend as milling time is increased.

3.3 *In-situ* Synchrotron Radiation Powder X-ray Diffraction study

The *in-situ* SR-PXD data of $NaAlH_4$-$Ca(BH_4)_2$ (1 h BM) is presented in Figure 3. Initially, the starting reactants, $NaAlH_4$ and $Ca(BH_4)_2$, are present in major fractions. The most intense Bragg reflections belonging to $NaBH_4$ are also present at *RT*, while no Bragg reflections from NaH, CaH_2 or Al are present, confirming reaction **1**. Indeed, Bragg reflections from $Ca(AlH_4)_2$ are not identified in the diffractogram at *RT*, however, $Ca(AlH_4)_2$ has previously been reported to be less crystalline and hence a relatively weak X-ray scatterer [11]. WC from the ball-milling is also present as a minor fraction in the sample with Bragg reflections present at 2θ = 16.7, 18.9 and 25.35°, however, the Bragg reflections overlap with $NaAlH_4$ and are thus difficult to distinguish.

Already at *T* = 33 and 60 °C the intensity of the Bragg reflections from $NaAlH_4$ and α-$Ca(BH_4)_2$, respectively, start to slowly decrease. Meanwhile, the intensity of $NaBH_4$ increases between 90 and 150 °C, indicating that reaction **1** is continuing during thermal treatment. At *T* = 130 °C, Bragg reflections from β-$Ca(BH_4)_2$ increase in intensity and reaches a maximum at *T* = 195 °C. Bragg reflections from α- and β-$Ca(BH_4)_2$ disappear at *T* = 237 and 320 °C, respectively. Additionally, Al begins to appear at *T* = 130 °C reaching maximum intensity at *T* = 229 °C while Bragg reflections from CaH_2 appear at *T* = 175 °C and reaches a maximum intensity at *T* = 237 °C. Finally, the most intense Bragg reflection from $NaAlH_4$ disappear at *T* = 211 °C.

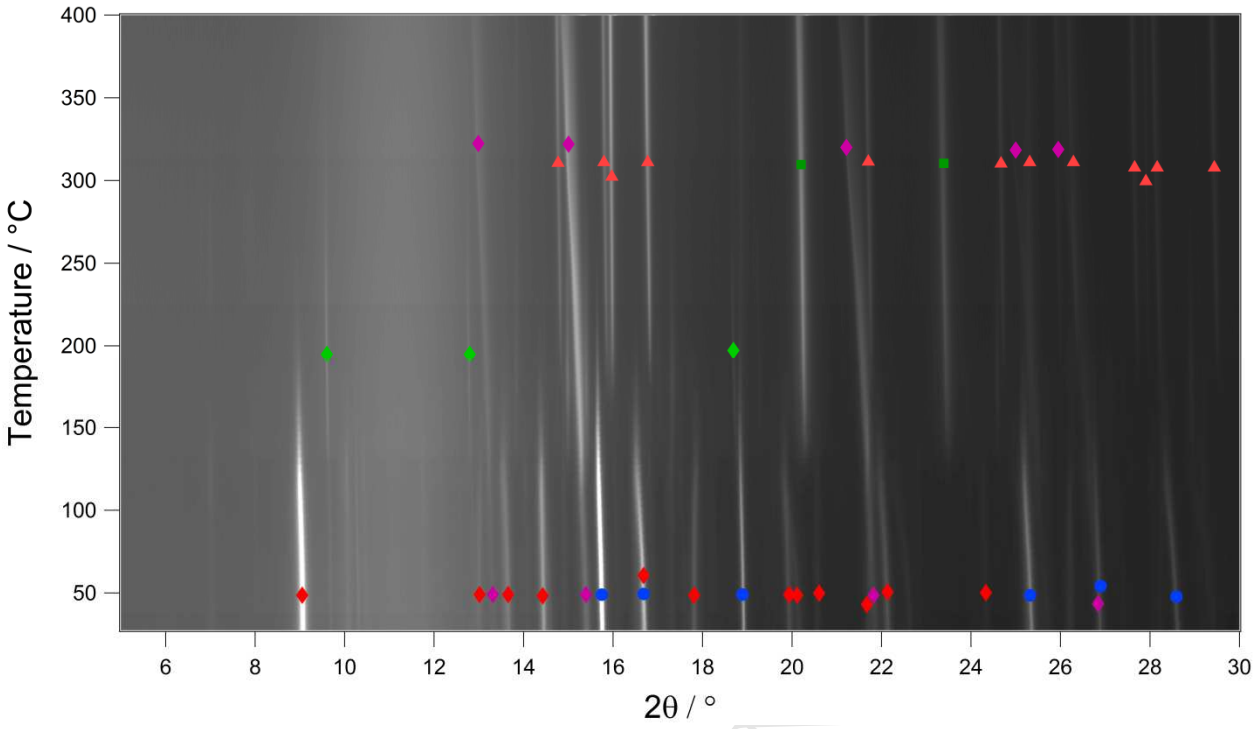

Figure 3. *In-situ* SR-PXD of $NaAlH_4$ - $Ca(BH_4)_2$ (BM 1 h) heated from *RT* to 400 °C ($\Delta T/\Delta t$ = 10 °C/min, λ = 0.8258 Å). Markers: Red diamonds: α-$Ca(BH_4)_2$, green diamonds: β-$Ca(BH_4)_2$, purple diamonds: $NaBH_4$, blue spheres: $NaAlH_4$, red triangles: CaH_2, green squares: Al.

3.4 Mass Spectrometry

The hydrogen release mechanism is presented for the sample mechanochemically treated for 6 h, since, as evident from PXD, reaction **1** has occurred to a larger extent (see Figure 4). MS data for the other samples can be seen in Figure S2 and S3. The first hydrogen release step initiates at *T* = 145 °C and peaks at 180 °C, whereas the second step initiates at *T* = 186 °C and reaches a maximum at 192 °C. The first two peaks are assigned to the decomposition of $Ca(AlH_4)_2$ [12]. As discussed earlier, the $NaAlH_4$ is reacting with $Ca(BH_4)_2$ according to reaction **1** upon heating, and it is believed that the conversion is full for the 6 hour BM sample.

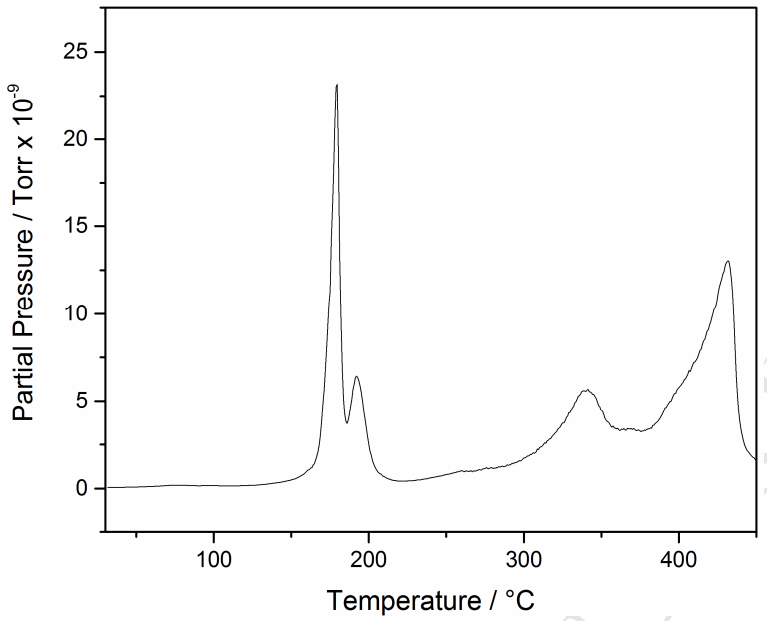

Figure 4. MS data (m/Z = 2) of $NaAlH_4$-$Ca(BH_4)_2$ (BM 6 h) showing H_2 release from RT to 450 °C ($\Delta T/\Delta t$ = 5 °C/min).

In comparison with the *in situ* SR-PXD data, where Al is observed at much lower temperature (T = 130 °C) than CaH_2 (T = 175 °C), the two step hydrogen release supports the suggested decomposition pathway [11,23]:

$Ca(AlH_4)_2$ (s) → $CaAlH_5$ (s) + Al (s) + 3/2H_2 (g) (**2**)

$CaAlH_5$ (s) → CaH_2 (s) + Al (s) + 3/2H_2 (g) (**3**)

The $M$$AlH_5$ decomposition intermediate has also been observed in the decomposition of $Sr(AlH_4)_2$ and $Eu(AlH_4)_2$ [24]. A minor hydrogen release is observed between T = 225 and 295 °C, which may be due to small amounts of $NaAlH_4$ reacting with $Ca(BH_4)_2$ to form $Ca(AlH_4)_2$, which immediately decomposes, or $NaAlH_4$ decomposing directly [25]. Finally, a more distinct hydrogen release is observed to begin at T = 295 °C with a peak at 340 °C before the final hydrogen release is initiated at T = 377 °C with a peak at 431 °C. The two final hydrogen release steps are assigned to decomposition of excess $Ca(BH_4)_2$ [26,27].

3.5 Sieverts' Measurement

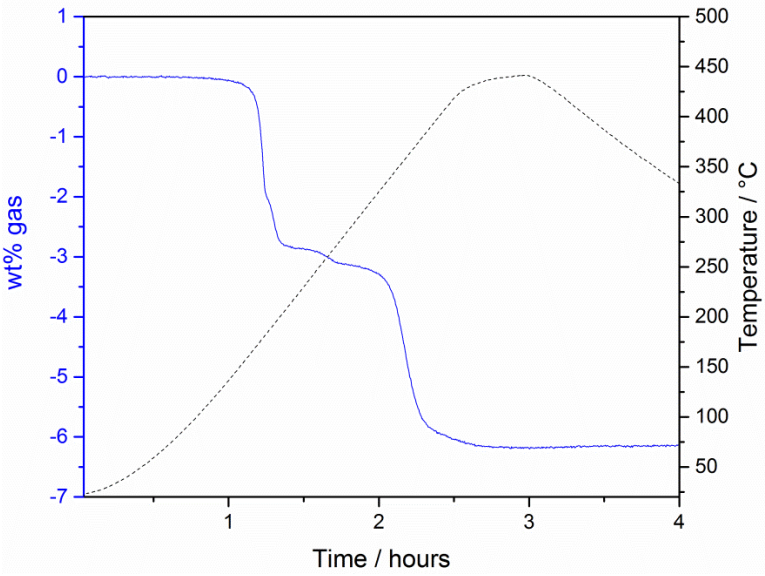

Figure 5. Sieverts' measurement of $NaAlH_4$-$Ca(BH_4)_2$ (BM 6 h) heated from *RT* to 450 °C ($\Delta T/\Delta t$ = 3 °C /min, $p(H_2)$ = 1 bar) and kept isothermal at 450 °C for 30 min.

The first gas release initiates at T = 120 °C releasing 2 wt% gas, while the second step begins at T = 185 °C releasing 0.8 wt% up to T = 220 °C. These two steps are in good agreement with the observations made by MS. Between 220 and 310 °C, an additional 0.35 wt% gas is released which is associated with the event also observed by MS in the same temperature range. Subsequently, a major release of 2.54 wt% gas is released between 310 and 385 °C before the final step initiates and releases an additional 0.44 wt% up to approximately 445 °C. Both steps are again associated with the decomposition of excess $Ca(BH_4)_2$. The total hydrogen release adds up to 6.1 wt%, which is in between the calculated hydrogen release from the $NaAlH_4$-$Ca(BH_4)_2$ (1:1) composite of 5.2 – 7.9 wt% depending on the degree of metathesis reaction, reaction scheme (1) (calculations provided in SI). A slight decrease of 0.3 wt% is observed between the samples ball-milled for 3 and 6 hours. Which may be due to decomposition of $Ca(AlH_4)_2$ during extended ball-milling. However, the decomposition products may not be observed in PXD due to small amounts combined with the decreased crystallinity after milling. The measured difference in hydrogen release may also be

related to the amount of sample used (0.1 g) as well as the volume change of the sample as the reaction and decomposition occur [28].

4. Conclusion

The composite system $NaAlH_4$-$Ca(BH_4)_2$ reacts according to reaction scheme **1** during mechanochemical treatment and prolongation of the ball-milling time leads to a higher degree of reaction. The presence of $Ca(AlH_4)_2$ was confirmed by FT-IR, whereas the decomposition temperature observed in MS is in good agreement with previously reported observations. Furthermore, reaction **1** may also be induced by thermal treatment as the reaction is observed to continue during heating in the *in-situ* SR-PXD experiment. Finally, a hydrogen release between 5.8 and 6.4 wt% was observed. Further exploration into the stoichiometric system $2NaAlH_4$-$Ca(BH_4)_2$ may provide a greater insight into this reactive hydride composite.

5. Acknowledgement

The work was supported by the Danish National Research Foundation, Center for Materials Crystallography (DNRF93), The Innovation Fund Denmark (project HyFill-Fast), Danish Council for Independent Research, DFF – 4181-00462 (HyNanoBorN), Energistyrelsen, EUDP (64013-0136), and the Danish Research Council for Nature and Universe (Danscatt). Finally, the authors are grateful to the Carlsberg Foundation.

6. References

[1] K.T. Møller, T.R. Jensen, E. Akiba, H. Li, Hydrogen - A sustainable energy carrier, Prog. Nat. Sci. Mater. Int. 27 (2017) 34–40.
[2] D.A. Sheppard, M. Paskevicius, T.D. Humphries, M. Felderhoff, G. Capurso, J.B. von Colbe, M. Dornheim, T. Klassen, P.A. Ward, J.A. Teprovich, C. Corgnale, R. Zidan, D.M. Grant, C.E. Buckley, Metal hydrides for concentrating solar thermal power energy storage, Appl. Phys. A. 122 (2016) 395.
[3] M.B. Ley, L.H. Jepsen, Y.-S. Lee, Y.W. Cho, J.M. Bellosta von Colbe, M. Dornheim, M. Rokni, J.O. Jensen, M. Sloth, Y. Filinchuk, J.E. Jørgensen, F. Besenbacher, T.R. Jensen, Complex hydrides for hydrogen storage – new perspectives, Mater. Today. 17 (2014) 122–128.

[4] L. Schlapbach, A. Züttel, Hydrogen-storage materials for mobile applications, Nature. 414 (2001) 353–358.
[5] Q. Lai, M. Paskevicius, D.A. Sheppard, C.E. Buckley, A.W. Thornton, M.R. Hill, Q. Gu, J. Mao, Z. Huang, H.K. Liu, Z. Guo, A. Banerjee, S. Chakraborty, R. Ahuja, K.-F. Aguey-Zinsou, Hydrogen Storage Materials for Mobile and Stationary Applications: Current State of the Art, ChemSusChem. 8 (2015) 2789–2825.
[6] B. Bogdanović, M. Schwickardi, Ti-doped alkali metal aluminium hydrides as potential novel reversible hydrogen storage materials, J. Alloys Compd. 253–254 (1997) 1–9.
[7] E. Rönnebro, E.H. Majzoub, Calcium Borohydride for Hydrogen Storage: Catalysis and Reversibility, J. Phys. Chem. B. 111 (2007) 12045–12047.
[8] Y. Filinchuk, E. Rönnebro, D. Chandra, Crystal structures and phase transformations in $Ca(BH_4)_2$, Acta Mater. 57 (2009) 732–738.
[9] C. Rongeat, V. D'Anna, H. Hagemann, A. Borgschulte, A. Züttel, L. Schultz, O. Gutfleisch, Effect of additives on the synthesis and reversibility of $Ca(BH_4)_2$, J. Alloys Compd. 493 (2010) 281–287.
[10] M. Paskevicius, L.H. Jepsen, P. Schouwink, R. Černý, D.B. Ravnsbæk, Y. Filinchuk, M. Dornheim, F. Besenbacher, T.R. Jensen, Metal borohydrides and derivatives – synthesis, structure and properties, Chem. Soc. Rev. 46 (2017) 1565–1634.
[11] M. Fichtner, C. Frommen, O. Fuhr, Synthesis and Properties of Calcium Alanate and Two Solvent Adducts, Inorg. Chem. 44 (2005) 3479–3484.
[12] M. Mamatha, B. Bogdanović, M. Felderhoff, A. Pommerin, W. Schmidt, F. Schüth, C. Weidenthaler, Mechanochemical preparation and investigation of properties of magnesium, calcium and lithium–magnesium alanates, J. Alloys Compd. 407 (2006) 78–86.
[13] R. Mohtadi, P. Sivasubramanian, S.-J. Hwang, A. Stowe, J. Gray, T. Matsunaga, R. Zidan, Alanate–borohydride material systems for hydrogen storage applications, Int. J. Hydrog. Energy. 37 (2012) 2388–2396.
[14] D.B. Ravnsbæk, T.R. Jensen, Tuning hydrogen storage properties and reactivity: Investigation of the $LiBH_4$–$NaAlH_4$ system, J. Phys. Chem. Solids. 71 (2010) 1144–1149.
[15] Y. Liu, Y. Yang, Y. Zhou, Y. Zhang, M. Gao, H. Pan, Hydrogen storage properties and mechanisms of the $Mg(BH_4)_2$–$NaAlH_4$ system, Int. J. Hydrog. Energy. 37 (2012) 17137–17145.
[16] H. Kabbour, C.C. Ahn, S.-J. Hwang, R.C. Bowman Jr., J. Graetz, Direct synthesis and NMR characterization of calcium alanate, J. Alloys Compd. 446–447 (2007) 264–266.
[17] K. Komiya, N. Morisaku, Y. Shinzato, K. Ikeda, S. Orimo, Y. Ohki, K. Tatsumi, H. Yukawa, M. Morinaga, Synthesis and dehydrogenation of $M(AlH_4)_2$ (M = Mg, Ca), J. Alloys Compd. 446–447 (2007) 237–241.
[18] K.T. Møller, M.B. Ley, P. Schouwink, R. Černý, T.R. Jensen, Synthesis and thermal stability of perovskite alkali metal strontium borohydrides, Dalton Trans. 45 (2015) 831–840.
[19] B.R.S. Hansen, K.T. Møller, M. Paskevicius, A.-C. Dippel, P. Walter, C.J. Webb, C. Pistidda, N. Bergemann, M. Dornheim, T. Klassen, J.-E. Jørgensen, T.R. Jensen, In situ X-ray diffraction environments for high-pressure reactions, J. Appl. Crystallogr. 48 (2015) 1234–1241.
[20] P.D. Pathak, N.G. Vasavada, Thermal expansion of NaCl, KCl and CsBr by X-ray diffraction and the law of corresponding states, Acta Crystallogr. Sect. A. 26 (1970) 655–658.
[21] Y.-W. Lee, B.M. Clemens, K.J. Gross, Novel Sieverts' type volumetric measurements of hydrogen storage properties for very small sample quantities, J. Alloys Compd. 452 (2008) 410–413.
[22] V. D'Anna, A. Spyratou, M. Sharma, H. Hagemann, FT-IR spectra of inorganic borohydrides, Spectrochim. Acta. A. Mol. Biomol. Spectrosc. 128 (2014) 902–906.

[23]M. Mamatha, C. Weidenthaler, A. Pommerin, M. Felderhoff, F. Schüth, Comparative studies of the decomposition of alanates followed by in situ XRD and DSC methods, J. Alloys Compd. 416 (2006) 303–314.
[24]A. Pommerin, A. Wosylus, M. Felderhoff, F. Schüth, C. Weidenthaler, Synthesis, Crystal Structures, and Hydrogen-Storage Properties of $Eu(AlH_4)_2$ and $Sr(AlH_4)_2$ and of Their Decomposition Intermediates, $EuAlH_5$ and $SrAlH_5$, Inorg. Chem. 51 (2012) 4143–4150.
[25]T.K. Nielsen, M. Polanski, D. Zasada, P. Javadian, F. Besenbacher, J. Bystrzycki, J. Skibsted, T.R. Jensen, Improved Hydrogen Storage Kinetics of Nanoconfined $NaAlH_4$ Catalyzed with $TiCl_3$ Nanoparticles, ACS Nano. 5 (2011) 4056–4064.
[26]J.-H. Kim, S.-A. Jin, J.-H. Shim, Y.W. Cho, Thermal decomposition behavior of calcium borohydride $Ca(BH_4)_2$, J. Alloys Compd. 461 (2008) L20–L22.
[27]M. Aoki, K. Miwa, T. Noritake, N. Ohba, M. Matsumoto, H.-W. Li, Y. Nakamori, S. Towata, S. Orimo, Structural and dehydriding properties of $Ca(BH_4)_2$, Appl. Phys. A. 92 (2008) 601–605.
[28]C.J. Webb, E.M. Gray, Analysis of the uncertainties in gas uptake measurements using the Sieverts method, Int. J. Hydrog. Energy. 39 (2014) 366–375.

Figure 1. Powder X-ray diffraction data of the $NaAlH_4$–$Ca(BH_4)_2$ samples after different degrees of mechanochemical treatment (λ = 1.5406 Å). Markers: Red diamonds: α-$Ca(BH_4)_2$, green diamonds: β-$Ca(BH_4)_2$, purple diamonds: $NaBH_4$, blue spheres: $NaAlH_4$.

Figure 2. FT-IR spectra of $NaAlH_4$-$Ca(BH_4)_2$ ball-milled at different ball-milling times.

Figure 3. *In-situ* SR-PXD of $NaAlH_4$ - $Ca(BH_4)_2$ (BM 1 h) heated from *RT* to 400 °C ($\Delta T/\Delta t$ = 10 °C/min, λ = 0.8258 Å). Markers: Red diamonds: α-$Ca(BH_4)_2$, green diamonds: β-$Ca(BH_4)_2$, purple diamonds: $NaBH_4$, blue spheres: $NaAlH_4$, red triangles: CaH_2, green squares: Al.

Figure 4. MS data (m/Z = 2) of $NaAlH_4$-$Ca(BH_4)_2$ (BM 6 h) showing H_2 release from RT to 450 °C ($\Delta T/\Delta t$ = 5 °C/min).

Figure 5. Sieverts' measurement of $NaAlH_4$-$Ca(BH_4)_2$ (BM 6 h) heated from *RT* to 450 °C ($\Delta T/\Delta t$ = 3 °C /min, $p(H_2)$ = 1 bar) and kept isothermal at 450 °C for 30 min.

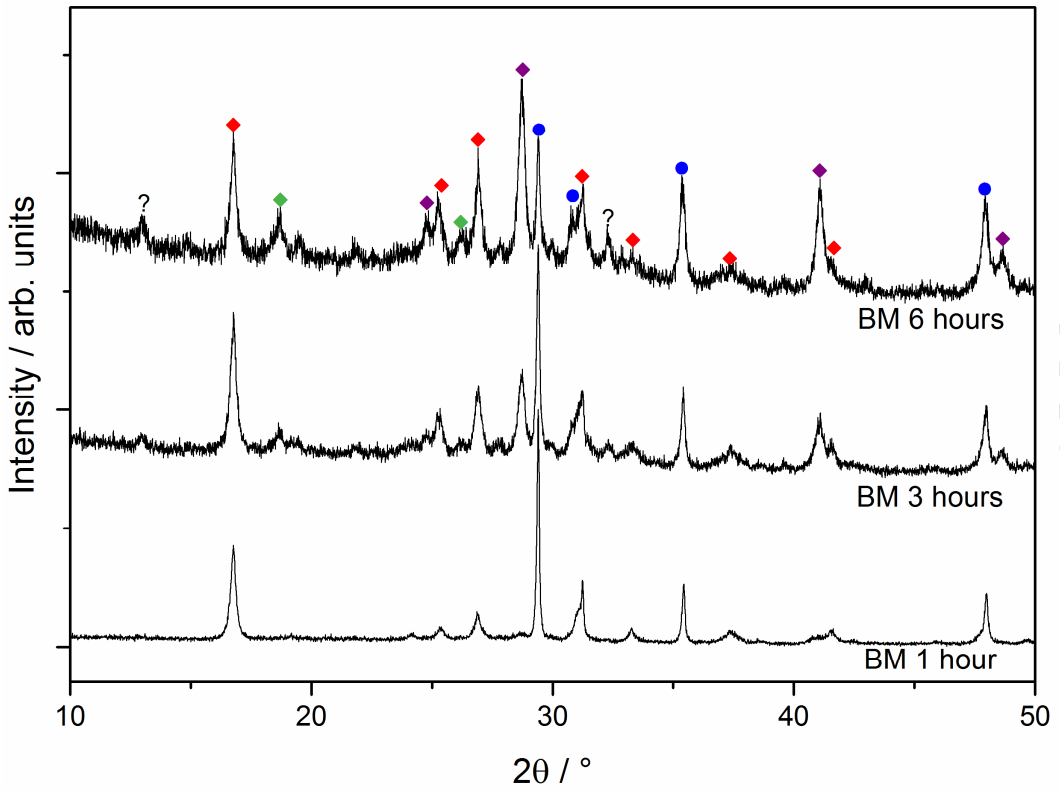

Fig. 1

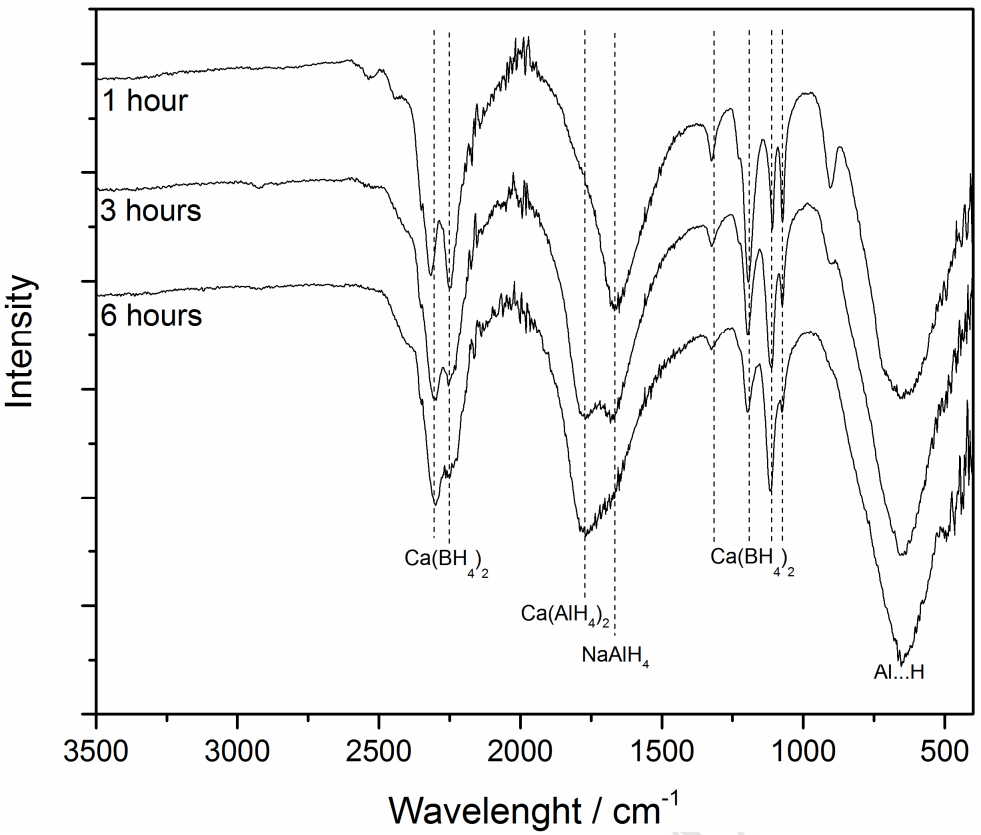

Fig. 2

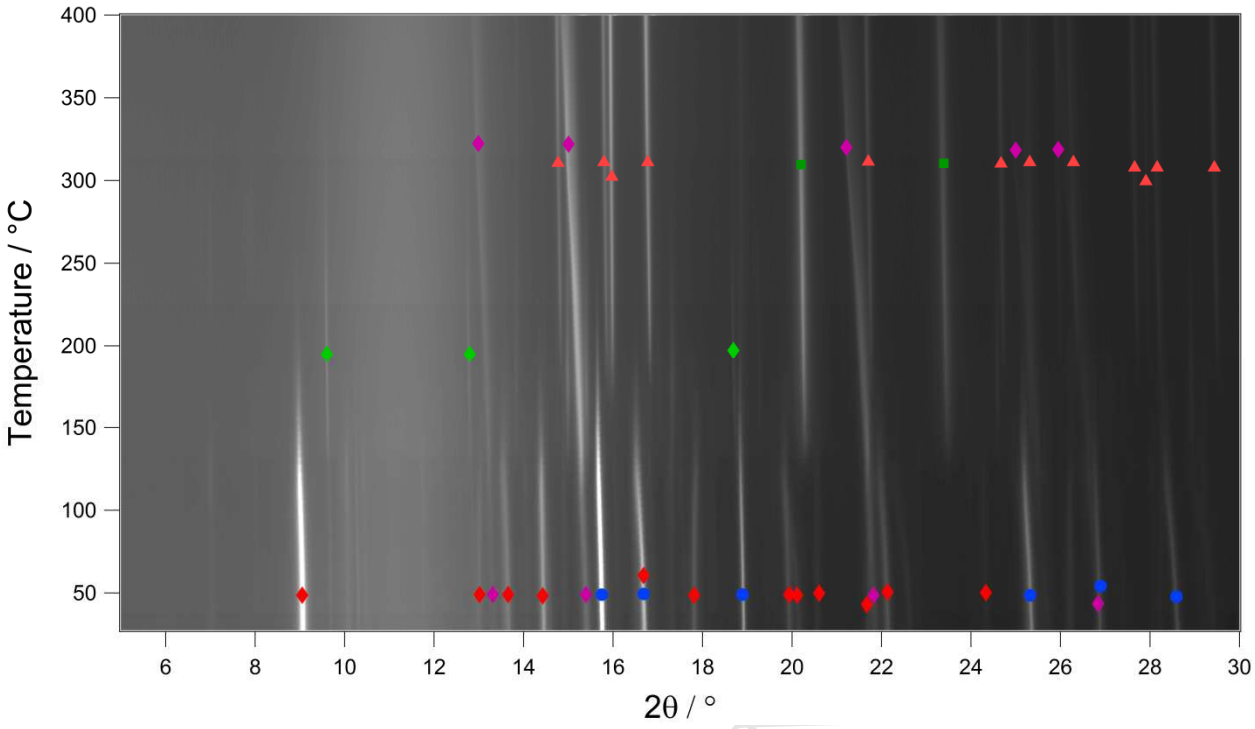

Fig. 3

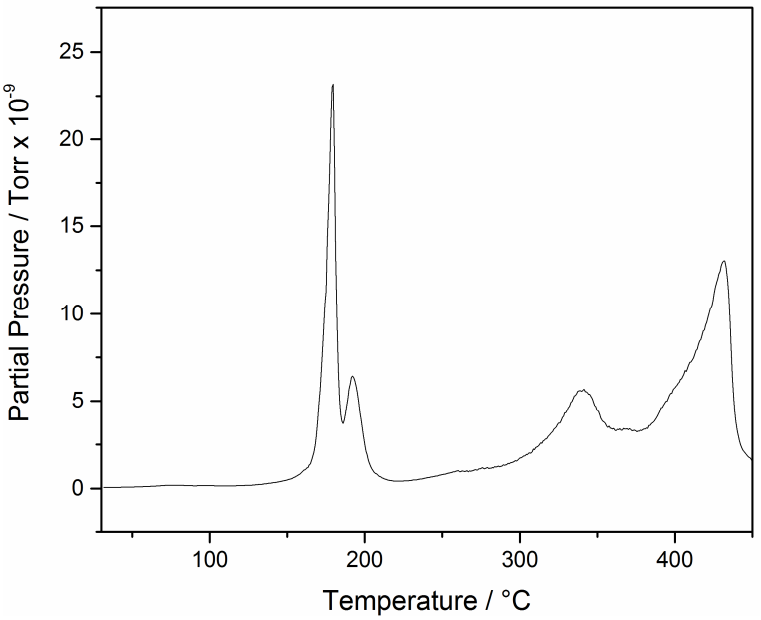

Fig. 4

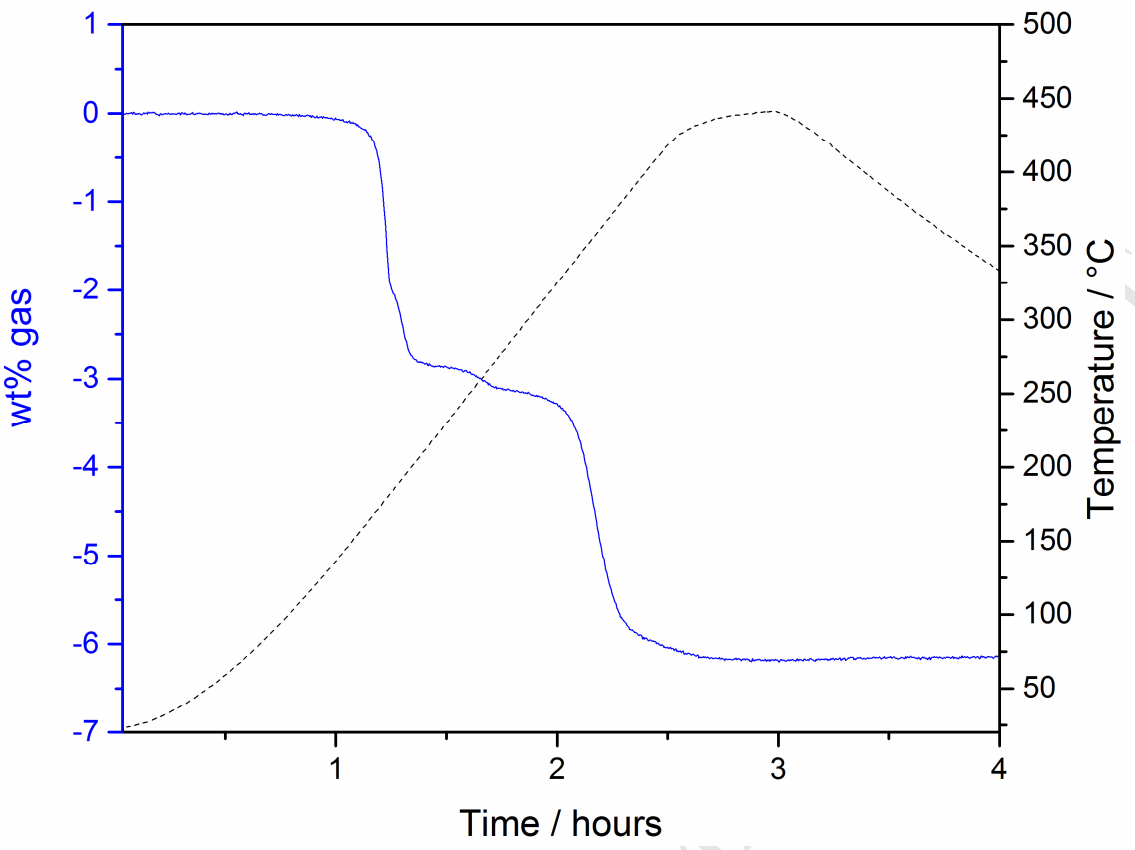

Fig. 5

Highlights

- $Ca(AlH_4)_2$ is formed in a metathesis reaction between $NaAlH_4$ and $Ca(BH_4)_2$.
- Increasing the ball-milling time increases the yield of $Ca(AlH_4)_2$.
- Thermal treatment enhances the metathesis reaction too.
- $Ca(AlH_4)_2$ decomposes in two steps below 200 °C releasing ~2.8 wt% H_2.

Highlights

- $Ca(AlH_4)_2$ is formed in a metathesis reaction between $NaAlH_4$ and $Ca(BH_4)_2$.
- Increasing the ball-milling time increases the yield of $Ca(AlH_4)_2$.
- Thermal treatment enhances the metathesis reaction too.
- $Ca(AlH_4)_2$ decomposes in two steps below 200 °C releasing ~2.8 wt% H_2.